Accepted 26/Dec/17 - 10.1021/acs.iecr.7b04584
Final version can be accessed through the ACS website

Overcoming the engineering constraints for scaling-up the state-of-the-art catalyst for tail-gas N_2O decomposition

Ignacio Melián-Cabrera,[†,Ⅲ]* Silvia Espinosa,[§] Cristina Mentruit,[§] Blaine Murray,[†,Ⅲ] Lorena Falco,[†] Joseph Socci,[†] Freek Kapteijn[§] and Jacob A. Moulijn[§]

† European Bioenergy Research Institute (EBRI), School of Engineering and Applied Science, Aston University, Aston Triangle, Birmingham, B4 7ET, United Kingdom.

Ⅲ Aston Institute of Materials Research, School of Engineering and Applied Science, Aston University, Aston Triangle, Birmingham, B4 7ET, United Kingdom.

§ Catalysis Engineering, Chemical Engineering Department, Delft University of Technology, Van der Maasweg 9, 2629 HZ Delft, The Netherlands.

KEYWORDS: environmental catalysis, scale-up, zeolites, N_2O emissions, greenhouse gases.

Accepted 26/Dec/17 - 10.1021/acs.iecr.7b04584
Final version can be accessed through the ACS website

GRAPHICAL ABSTRACT

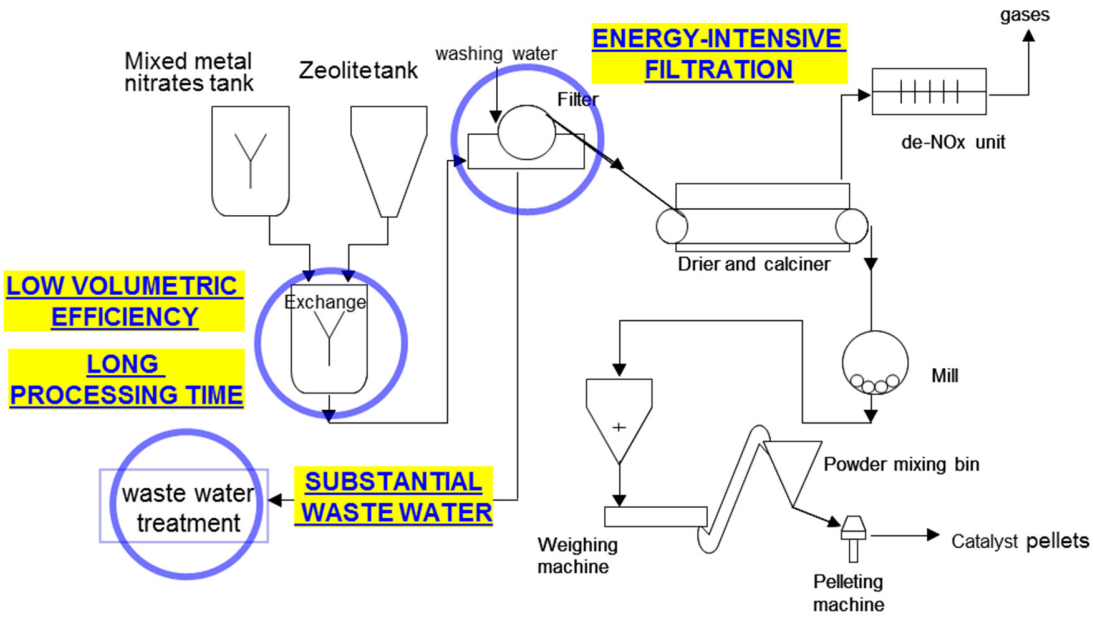

Accepted 26/Dec/17 - 10.1021/acs.iecr.7b04584
Final version can be accessed through the ACS website

ABSTRACT

An efficient process is reported for preparing a state-of-the-art Fe-ferrierite catalyst for N_2O decomposition under industrial tail-gas conditions. In the synthesis procedure we evaluate the very demanding constraints for scale-up; *i.e.* large reactor volumes are typically needed, long processing times and considerable amounts of waste water is generated. The proposed synthesis minimizes the amount of water used, and therefore the amount produced waste water is minimal; in this approach there is no liquid residual water stream that would need intensive processing. This has remarkable benefits in terms of process design, since the volume of equipment is reduced and the energy-intensive filtration is eliminated. This route exemplifies the concept of process intensification, with the ambition to re-engineer an existing process to make the industrial catalyst manufacture more sustainable. The so-obtained catalyst is active, selective and very stable under tail gas conditions containing H_2O, NO and O_2, together with N_2O; keeping a high conversion during 70 h time on stream at 700 K, with a decay of 0.01%/h, while the standard reference catalyst decays at 0.06%/h; hence it deactivates six times slower, with ~5% absolute points of higher conversion. The excellent catalytic performance is preliminary ascribed to the differential speciation.

1. Introduction

The decomposition of N_2O into N_2 and O_2 is a reaction with proven environmental benefits.[1,2] The greenhouse warming potential (GHWP) of N_2O is 250-300 higher than that of CO_2,[3] which means that eliminating relatively small N_2O gas emissions will have a large impact in terms of CO_2 equivalent reduction, as compared to CH_4 (GHWP of 28-36). Moreover, N_2O plays a role in ozone depletion. N_2O gas is principally emitted from anthropogenic sources; agriculture and chemical industry being the major sources. The chemical industry contributes in two major areas, viz., as by-products of adipic and nitric acid production. An attractive approach to synthesize N_2O-free adipic acid has been proposed by a photochemistry based approach using ozone and UV light,[4] but currently the major adipic acid producers still apply cost-effective N_2O abatement technologies or NOx/N_2O retrofitting into the nitric acid process.[5] Also in the case of nitric acid production plants, it is expected that these abatement routes will play a major role in the future, since retrofitting in existing plants will be needed for at least several decades. Several options have been claimed to deal with this. Metal oxide-based catalysts have been proposed for high temperature operation conditions, for instance below the Pt-Rh gauzes in the ammonia oxidation reactors.[6,7] End-of-pipe catalysed direct N_2O decomposition has been recognized as an economically feasible option, in existing plants and it does not modify the nitric acid production.[8]

This work deals with the constraints to scale-up a state-of-the-art catalyst, leading to a new catalyst synthesis concept for the N_2O decomposition reaction under industrial tail-gas conditions. Ferrierite has been recognized as the most active zeolite support in combination with Fe species for this reaction under end-of-pipe conditions. The catalyst is prepared in such a way

that the methodology can be considered optimal for scale-up, and can be embedded in the green chemistry[9] and process intensification principles.[10] Due to the carefully-selected synthesis conditions, the overall process is simplified significantly in terms of less steps required, and reduced size of equipment.

The N_2O decomposition reaction can be catalysed by Fe-based zeolites, such as ZSM-5,[11-15] Ferrierite,[16-19] beta[11,19-23] and TNU/IM-type zeolites.[24] Various methods have been proposed for Fe incorporation, including wet-ion exchange, solid-state ion exchange, isomorphous substitution, steaming, chemical vapour deposition, among others. Wet-ion exchange is a simple methodology where a Fe-salt, dissolved in water, is contacted with the zeolite and Fe(II)/Fe(III) cations are exchanged on the Brønsted sites resulting in a Fe-exchanged zeolite.

Wet-ion exchange appears to be the simplest procedure commercially, resulting in a reproducible methodology. Various disadvantages, however, appear when the process would be scaled-up. Figure 1 shows a simplified process flow diagram for a metal-exchanged zeolite production facility based on wet ion exchange. The major drawbacks are highlighted as follows: 1) large volumetric reactors are needed; typically liquid/solid ratios higher than 5 kg_{liquid}/kg_{solid} are used, implying the need of large-volume reactors or, in other words, the conventional reactors work at a low volumetric efficiency; 2) the ion-exchange involves long processing times of around 10 to 24 h, which makes the process discontinuous; 3) a large amount of waste water is formed during the exchange, washing and filtering of the exchanged zeolite. As an example, for producing 10 t/day of catalyst, the generated waste water is around 50 m^3/day for the exchange only.[25] Such amount of produced waste water requires extra equipment for storage, and most importantly,

the water has to be treated before disposal to the surface water or municipal sewer system; usually nitrates are extensively present and denitrification based on bacterial degradation is commonly applied that makes the process costly.[26] Finally, 4) filtration is energy intensive, with high processing costs due to the small size of the zeolite grains. Based on the above reasoning, new catalyst synthesis strategies for addressing these bottlenecks are to be developed, which is the basis of this work.

2. Experimental

2.1 Chemicals

The used chemicals are HNO_3, Merk 65.0 *wt*.%; $Fe(NO_3)_3.9H_2O$, Acros 99.0 % metal basis; NH_4NO_3, Merk extra pure; hydrofluoric acid, Merk 40%. Ferrierite was kindly supplied by Tosoh, with material reference 720 KOA. Fe(III)-nitrate was chosen because it is typically the lowest-cost Fe salt precursor, while NH_4NO_3 was employed due to the easy elimination of the NO_3^- in the downstream processing with a deNOx unit.

2.2 Zeolite pre-treatment

The as-received commercial zeolite having an FER structure[27] is in the sodium-potassium form, and is formed by agglomerates of platelets and cylinders of different sizes and shapes. The average particle size ranges from 0.5 to 2 μm as determined by SEM, Figure 2. The sample was exchanged twice with a NH_4NO_3 solution to get the ammonium form: once using a saturated solution (2.0 M at 353 K for 24 h) and then a milder exchange was applied (1.0 M same temperature and time). Between the ammonium treatments, the sample was filtered and washed repeatedly with distilled water to remove residual Na^+ and K^+. The effectiveness of this

exchange procedure was verified by ICP elemental analysis, as reported in Table 1. Cation exchange efficiencies of >99.9% for Na^+ and 99.8% for K^+ were obtained. We should note that this step is unavoidable. If the Fe(III) exchange is carried out on the Na/K form zeolite, the Fe cations would precipitate due to the high pH, resulting in a poor catalyst performance.

This step also produces quite some residual water, which could be optimized using the same concept as described here for the Fe-zeolite preparation. However, at this stage we found the NH_4NO_3 washing step less attractive academically, compared with the Fe-exchange itself. Thus, the overall process is not yet fully optimized.

2.3 Catalyst preparation

2.3.1 Reference standard catalyst

The reference standard catalyst was prepared identically to the method described by Melian-Cabrera *et al*.[17]

2.3.2 Static mode

The $Fe(NO_3)_3$ solution was prepared considering the total pore volume of the zeolite with a slight excess; the concept of the 'total liquid pore volume' is illustrated in Figure 3. In total, a ratio of 2.5 ml solution/g zeolite was employed. The pH was adjusted in the following way. Milli-Q water was adjusted to pH = 2 using diluted HNO_3. The Fe-precursor was added to this solution, and the resulting solution was added to the NH_4-zeolite (described in 2.2). The exchange was performed at three increasing ageing times: 1, 6 and 24 h, resulting in three different samples. The preparation was carried out at room

temperature and after the Fe-exchange, water was removed by heating the sample at 363 K in a stove furnace overnight.

2.3.3 Dynamic mode

The procedure is very similar to the previous one. The solution was prepared in the same way, but after adding the zeolite, the sample was continuously stirred by means of a 2D shaker, as shown in Figure 3B. The ageing time was varied for 1, 6 and 24 h, resulting in three different samples. After the exchange, all the water was evaporated using a rota-evaporator set-up at 353 K.

2.4. Calcination

All the catalysts were calcined at 723 K for 4 h, prior to the activity tests.

2.5 Catalyst characterization

The elemental content of Na, K, Fe, Si and Al was determined by ICP, of the previously dissolved zeolites in a 6 *wt.*% HF solution, using a Perkin-Elmer Optima 3000DV.

SEM pictures were recorded with a Philips Scanning Electron Microscope (XL 20) at 10 kV. The sample was *sputtered* with gold three times using a standard gas plate metallizing chamber.

Temperature-programmed reduction with H_2 was performed in a Micromeritics TPD/TPR 2900 apparatus, using a high purity mixture of 10 *vol.*% H_2 in Ar as reducing mixture. A cold trap was used to remove the water stemming from the reduction before the gas of the reactor outlet was sent to the TCD. The experimental conditions were carefully chosen via the characteristic parameter P ($P = \beta \cdot S_o$) / ($\phi_v \cdot C_o$)), where: S_o is the initial amount of reducible oxide (mol), ϕ_v the total flow rate (cm^3/min), β the heating rate (K/min) and C_o the initial H_2 concentration (mol/cm^3).

The *P* parameter was smaller than 1 K, which is very conservative as compared to the recommended $P \leq 20$ K by Malet and Caballero.[29]

2.6 Catalytic activity tests

The activity tests were carried out in a parallel six-flow reactor set-up using approximately 50 mg of 125-250 μm catalyst particles. The applied conditions are as follows: 4.5 mbar N_2O of a N_2O/He mixture at a total pressure of 3 bar absolute, a space time of ~900 kg·s/mol ($W/F^O(N_2O)$ where W is the catalyst mass and $F^O(N_2O)$ the molar flow of N_2O in the feed). The reactor outlet stream was analyzed on-line by gas chromatography; Chrompack CP 9001 equipped with a Poraplot Q column (for N_2O and N_2/O_2 separation) and a Molsieve 5A column (for N_2 and O_2). Helium is used as carrier gas in the GC analysis instead of nitrogen in order to detect the nitrogen produced in the reaction. The catalysts were pretreated in a flow of He at 673 K for 1 h prior the reaction, and cooled down in the same gas to the starting reaction temperature. Steady state was achieved after 1 h on-stream, since the composition of the product flows were constant.

The catalyst was also tested under nitric acid-based tail gas conditions with the following composition: 4.5 mbar N_2O, 0.6 mbar NO, 15 mbar H_2O and 75 mbar O_2, maintaining the same space time $W/F^O(N_2O)$ of ~900 kg·s/mol at 3 bar(a) of total pressure. The feed is simulated by adding these components from more concentrated mixtures in helium. Stability tests were carried out under these conditions at 700 K for 70 h time on stream.

3. Results and discussion

The preparation method is based on the 'total liquid pore volume' concept ($V^{T\text{-}LIQ}$) to reach the caking end-point.[28] The amount of solution used for exchange is enough to fill the $V^{T\text{-}LIQ}$ of the material; for practical purposes a slight excess of liquid is used resulting in a liquid/solid = 2.5 (ml/g). The excess of water is necessary to allow the mixing of the material during the exchange and, in practice, making easier its handling. The low liquid use implies that the filtration step in Figure 1 can be eliminated, simplifying the overall process scheme and reducing the operational costs. In Figure 3, the typical experimental set-up is shown, where a two-dimensional shaker was employed in order to homogenize the so-obtained slurry. Since the method uses a minimal amount of water, this can be easily evaporated, while the anions are left on the zeolite's surface. These anions decompose during the drying and calcination, and in a deNOx unit the produced NO_x is reduced into N_2. Overall, this strategy avoids a large volume of nitrates containing waste water, which would require denitrification with bacterial broths, which is energy intensive and costly as reported elsewhere.[26] The amount of water used is two times lower compared to the amount of water used in the most effective method in patent literature.[25]

The preparation rheology was the first studied parameter. Two variants were considered: a static versus a dynamic exchanging procedure. The main difference between them is that for the dynamic mode the slurry is shaken during the exchange, while the other variant is fully static. The results of the catalysts prepared by these two variants are presented in Figure 4 and 5; representing the N_2O conversion as a function of the reaction temperature. The graphs include various catalyst samples prepared at increasing exchange time (*i.e.* 1, 6 and 24 h). A benchmarked Fe-FER catalyst having similar Fe loading, which gave excellent results in terms of activity and

stability, was used as reference standard.[17] This reference catalyst is the most active for this reaction under end-of-pipe conditions;[16,17,25] it was prepared in house by wet-ion exchange of iron nitrate at pH of 2.5 with 0.5 *wt.* % nominal loading of iron.

Results of the static-based catalysts do show quite some differences in the activity profiles (Figure 4). For long exchange time (24 h), the activity decreased considerably. For exchange times of 1 and 6 h the catalysts show similar levels of N_2O conversion, which were always below the performance of the reference catalyst. Because of the lower N_2O conversion than the reference catalyst, a dynamic variant was investigated subsequently.

The results are different for the dynamic wetness impregnation (Figure 5). Similar activity levels were achieved for all the exchange times. It should be noted that the activity of all these catalysts was as good as that of the reference catalyst, and more active than the static counterparts. No significant differences by increasing the exchange time were found; it means that it is possible to achieve a highly active N_2O decomposition catalyst by using a short exchange time with small liquid volumes.

An interpretation for the differences between dynamic and static conditions could be found in the mass transfer: under stirred conditions concentration gradients in the slurry may cancel out, improving the concentration distribution over the particles. Whereas under the static mode, the metal deposition could further be occurring unevenly due to agglomerate formation.

The optimal Fe-FER catalyst (dynamic, 1 h) was tested under practical conditions of the nitric acid plant tail-gases. These conditions are more appropriate than only in N_2O/He in order to evaluate its applicability as an end-of-pipe catalytic technology. Typical gases and concentrations found in

tail gases of nitric acid plants are NO (200 ppm), O_2 (2.5 *vol.*%) and H_2O (0.5 *vol.*%) together with N_2O (1500 ppm). Figure 6 presents the N_2O conversion for the optimal Fe-FER catalyst both in N_2O/He and in the presence of tail gas components. The presence of tail-gas components has no significant impact on the catalyst performance. The activity obtained under tail gas conditions was only slightly lower than with pure N_2O/He; a very positive result. Previous investigations on the effect of every individual component revealed a clear promoting effect of NO, counterbalanced by water inhibition, while O_2 has a neutral impact.[17]

The stability of the catalyst was further investigated by an isothermal test under tail gas conditions with increasing time on stream (TOS) up to 70 h. In Figure 7 the stability is compared with the reference catalyst. The obtained results are excellent; the optimal catalyst keeps a high conversion during the whole period of time, with a decay of only 0.01%/h, while the reference catalyst decays at a rate of 0.06%/h; *i.e.* the optimal catalyst deactivates six times slower over the same TOS range. A second finding is that the optimal catalyst yields ~5% absolute points of higher conversion than the reference catalyst.

Preliminary characterization shows that the Fe content was close to the nominal value, 0.47 *wt.*% Fe and the Si/Al ratio was 8.7. The slightly lower Fe loading than the theoretical value 0.50 *wt.*% can be explained by the H^+/Fe^{3+} competition during the exchange; as discussed elsewhere.[30] The Si/Al ratio is comparable to that of the as-received zeolite material (8.9). Temperature-programmed reduction (TPR) characterization shed some light on the type of Fe species formed during exchange, on both the optimal and reference catalysts. The TPR profiles for both catalysts reveal two clear reduction peaks at low temperatures, at ~600 and ~700 K (Figure 8). This region

corresponds to the reduction of the Fe^{3+} in exchanged positions (cations and oxocations) on the zeolite framework.[16] The optimal catalyst shows a fraction of Fe_2O_3 species, represented by the broad peak centred at 800 K,[30] that accounts for *ca.* 10% of the Fe, based on a TPR quantification method for Fe-zeolites.[31] The presence of only such a small Fe_2O_3 fraction is unexpected thermodynamically, if we take into account that the concentration of the used Fe solution was 100 times higher than the solution used for the reference catalyst: 3.71×10^{-2} M versus 3.71×10^{-4} M, respectively. In view of the solubility at pH = 2 of 2.7×10^{-3} M (using K_{SP} = 2.7×10^{-39}),[32] precipitation of $Fe(OH)_3$ is thermodynamically expected for our catalyst synthesis conditions. Apparently, the kinetics of the Fe^{3+} exchange is faster than the $Fe(OH)_3$ precipitation.

Several groups have evidenced that TPR provides relevant information on the Fe species present. Guzmán-Vargas *et al.*[16] compared the performance of Fe-BEA, -ZSM-5 and -FER catalysts with TPR results. They found for FER the largest amounts of "oxo-species" reducible at low temperature. This was confirmed by Jíša *et al.*[33] who also reported a correlation between the low-temperature reduction and the N_2O conversion; in both studies the dissociation of N_2O was studied under model conditions, *i.e.* not under realistic tail gas conditions.

The TPR patterns (Figure 8) evidence the presence of Fe-exchanged active species, namely those reduced at ~600 and ~700 K, for the optimal catalyst as well as for the reference catalyst (and some Fe_2O_3 species for the optimal catalyst). The optimal catalyst has a different Fe speciation than the reference catalyst, with more of the 700 K species; this is tentatively attributed to a difference in distribution of the optimal active sites. This suggests that the second Fe species reduction peak may represent the most optimal active sites. The sites reduced at lower

temperature are also active, otherwise the reference catalyst would not be about equally active. Ultimately, the FeOx peak probably does not represent sites with a high activity since it has a low intrinsic activity.[11]

4. Conclusions

A synthesis strategy of Fe-Ferrierite, the state-of-the-art tail gas N_2O decomposition catalyst, has been proposed circumventing constraints for scale-up. The method minimizes the amount of waste water produced and this has benefits from the process design point of view. The catalyst synthesis method utilizes only slightly more water compared to the total liquid pore volume of the zeolite. Consequently, it does not produce waste water that would require intensive processing. The catalyst shows excellent performance under end-of-pipe nitric acid conditions, which is attractive for retrofitting existing plants, with potential substantial savings in greenhouse gas emissions. In terms of process design, the proposed route simplifies the scale-up since the required equipment will be smaller (ion-exchange reactor) or can be avoided (filtration step). Further, the processing costs will be lower due to the low exchange times, and the elimination of filtration costs that are often considerable due to the small size of the zeolite grains.

AUTHOR INFORMATION

Corresponding Author: i.melian-cabrera@aston.ac.uk (Ignacio V. Melián Cabrera)

ACKNOWLEDGMENTS

This work was supported by the European Commission (HPMF-CT-2002-01873) started in Delft University of Technology and completed in EBRI, Aston University. B.M., L.F. and J.S. thank the School of Engineering and Applied Science, Aston University, for financial support.

REFERENCES

(1) Kapteijn, F.; Rodriguez-Mirasol, J.; Moulijn, J.A. Heterogeneous catalytic decomposition of nitrous oxide. *Appl. Catal. B: Environ.* **1996**, 9, 25-64.

(2) Zhang, R.; Liu,N.; Lei, Z.; Chen, B. Selective Transformation of Various Nitrogen-Containing Exhaust Gases toward N_2 over Zeolite Catalysts. *Chem. Rev.* **2016**, 116, 3658-3721.

(3) URL:https://www.epa.gov/ghgemissions/understanding-global-warming-potentials, accessed on 26-10-2017.

(4) Hwang, K.C.; Sagadevan, A. One-pot room-temperature conversion of cyclohexane to adipic acid by ozone and UV light. *Science.* **2014**, 346, 1495-1498.

(5) Schneider, L.; Lazarus, M.; Kollmuss, A. Industrial N_2O projects under the CDM: Adipic acid - A case of carbon leakage? *Working paper WP-US-1006*, Stockholm Environment Institute, Somerville, MA, **2010**.

(6) Santiago, M.; Pérez-Ramírez, J. Decomposition of N_2O over hexaaluminate catalysts, *Environ. Sci. Tech.* **2007**, 41, 1704-1709.

(7) Konsolakis M. Recent Advances on Nitrous Oxide (N_2O) Decomposition over Non-Noble-Metal Oxide Catalysts: Catalytic Performance, Mechanistic Considerations, and Surface Chemistry Aspects, *ACS Catal.* ***2015***, 5, 6397−6421.

(8) Perez-Ramirez, J; Kapteijn, F.; Schöffel, K.; Moulijn, J.A. Formation and control of N_2O in nitric acid production: Where do we stand today? *Appl. Catal. B: Environ.* **2003**, 44, 117-151.

(9) P.T. Anastas, J.C. Warner, Green Chemistry: Theory and Practice, Oxford University Press, **2000**.

(10) A. Stankiewicz, J.A. Moulijn, Re-Engineering the Chemical Processing Plant: Process Intensification, CRC Press, **2003**.

(11) Pieterse, J.A.Z.; Booneveld, S.; van der Brink, R. Evaluation of Fe-zeolite catalysts prepared by different methods for the decomposition of N_2O. *Appl. Catal. B: Environ.* **2004**, 51, 215-228.

(12) Pérez-Ramírez, J.; Kapteijn, F.; Mul, G.; Moulijn, J.A. Superior performance of ex-framework FeZSM-5 in direct N_2O decomposition in tail-gases from nitric acid plants. *Chem. Commun*. **2001**, 693-694.

(13) Pirngruber, G.D.; Luechinger, M.; Roy, P.K.; Cecchetto, A.; Smirniotis, P. N_2O decomposition over iron-containing zeolites prepared by different methods: a comparison of the reaction mechanism. *J. Catal*. **2004**, 224, 429–440.

(14) Zhu, Q.; van Teeffelen, R.M.; van Santen, R.A.; Hensen, E.J.M.; Effect of high-temperature treatment on Fe/ZSM-5 prepared by chemical vapor deposition of $FeCl_3$ II. Nitrous oxide decomposition, selective oxidation of benzene to phenol, and selective reduction of nitric oxide by isobutene. *J. Catal*. **2004**, 221, 575–583.

(15) Roy, P.K.; Prins, R.; Pirngruber, G.D. The effect of pretreatment on the reactivity of Fe-ZSM-5 catalysts for N_2O decomposition: Dehydroxylation vs. steaming. *Appl. Catal. B: Environ*. **2008**, 80, 226-236.

(16) Guzmán-Vargas, A.; Delahay, G.; Coq, B. Catalytic decomposition of N_2O and catalytic reduction of N_2O and N_2O + NO by NH_3 in the presence of O_2 over Fe-zeolite. *Appl. Catal. B: Environ*. **2003**, 42, 369-379.

(17) Melián-Cabrera, I.; Mentruit, C.; Pieterse, J.A.Z.; van den Brink, R.W.; Mul, G.; Kapteijn, F.; Moulijn, J.A. Highly active and stable ion-exchanged Fe–Ferrierite catalyst for N_2O decomposition under nitric acid tail gas conditions. *Catal. Commun.* **2005**, 6, 301-305.

(18) Melián-Cabrera, I.; Espinosa, S.; García-Montelongo, F.J.; Kapteijn, F.; Moulijn, J.A. Ion exchanged Fe-FER through H_2O_2-assisted decomplexation of organic salts. *Chem. Commun*., **2005**, 1525-1527.

(19) Kaucký, D.; Sobalík, Z.; Schwarze, M.; Vondrová, A.; Wichterlová, B. Effect of FeH-zeolite structure and Al-Lewis sites on N_2O decomposition and NO/NO_2-assisted reaction. *J. Catal*. **2006**, 238, 293-300.

(20) Pérez-Ramírez, J., Groen, J.C.; Brückner, A.; Kumar, M.S.; Bentrup, U.; Debbagh, M.N.; Villaescusa, L.A. Evolution of isomorphously substituted iron zeolites during activation: comparison of Fe-beta and Fe-ZSM-5. *J. Catal.* **2005**, 232, 318-334.

(21) Melián-Cabrera, I.; Kapteijn, F.; Moulijn, J.A. One-pot catalyst preparation: combined detemplating and Fe ion exchange of BEA through Fenton's chemistry. *Chem. Commun.* **2005**, 2178-2180.

(22) Liu, N.; Zhang, R.; Chen, B.; Li, Y.; Li, Y. Comparative study on the direct decomposition of nitrous oxide over M (Fe, Co, Cu)–BEA zeolites. *J. Catal.* **2012**, 294, 99-112.

(23) Rutkowska, M.; Chmielarz, L.; Macina, D.; Piwowarska, Z.; Dudek, B.; Adamski, A.; Witkowski, S.; Sojka, Z.; Obalová, L.; Van Oers, C.J.; Cool, P. Catalytic decomposition and reduction of N_2O over micro-mesoporous materials containing Beta zeolite nanoparticles. *Appl. Catal. B: Environ.* **2014**, 146, 112–122.

(24) Lee, J.K.; Kim, Y.J.; Lee, H.; Kim, S.H.; Cho, S.J.; Nam, I.; Hong, S.B. Iron-substituted TNU-9, TNU-10, and IM-5 zeolites and their steam-activated analogs as catalysts for direct N_2O decomposition. *J. Catal*. **2011**, 284, 23-33.

(25) Neveu, B.; Hamon, C.; Malefant, K. French Patent WO **99**/34901. Example 1.

(26) J.H. Mark, J.H. Jr Mark, "Water and Wastewater Technology", 5th Ed., Pearson Prentice Hall, Ohio, **2004**.

(27) Ch. Baerlocher and L.B. McCusker, Database of Zeolite Structures: http://www.iza-structure.org/databases/; accessed on 26-10-2017.

(28) Innes, W.B. Total Porosity and Particle Density of Fluid Catalysts by Liquid Titration. *Anal. Chem*. **1956**, 28, 332-334.

(29) P. Malet, A. Caballero, J. Chem. Soc., Faraday Trans. 1. 84 (1988) 2369-2375.

(30) Melián-Cabrera, I.; van Eck, E.R.H.; Espinosa, S.; Siles-Quesada, S.; Falco, L.; Kentgens, A.P.M.; Kapteijn, F.; Moulijn, J.A. Tail gas catalyzed N_2O decomposition over Fe-beta zeolite. On the promoting role of framework connected AlO_6 sites in the vicinity of Fe by controlled dealumination during exchange. *Applied Catal. B: Environ*. **2017**, 203, 218-226.

(31) Melián-Cabrera, I.; Espinosa, S.; Groen, J.C.; van der Linden, B.; Kapteijn, F.; Moulijn, J.A. Utilizing full-exchange capacity of zeolites by alkaline leaching: Preparation of Fe-ZSM5 and application in N_2O decomposition. *J. Catal.* **2006**, 238, 250-259.

(32) Haynes, W.M. Ed., Handbook of Chemistry and Physics, 97th ed.; CRC Press: Boca Raton, FL, **2017**.

(33) Jíša, K.; Nováková, J.; Schwarze, M.; Vondrová, A.; Sklenák, S.; Sobalik, Z. Role of the Fe-zeolite structure and iron state in the N_2O decomposition: Comparison of Fe-FER, Fe-BEA, and Fe-MFI catalysts. *J. Catal.* **2009**, 262, 27–34.

Accepted 26/Dec/17 - 10.1021/acs.iecr.7b04584
Final version can be accessed through the ACS website

FIGURES AND TABLES

Accepted 26/Dec/17 - 10.1021/acs.iecr.7b04584
Final version can be accessed through the ACS website

Table 1. Na and K content before and after ion exchange NH_4-treatment of the parent ferrierite.

Material	Na	K
As-received [a]	1.2 *wt.* %	1.2 *wt.* %
After NH_4-treatment	< 10 ppm (99.9)[b]	82 ppm (99.8)[b]

[a] Commercial specifications
[b] Values between parentheses are the cation exchange efficiency (%).

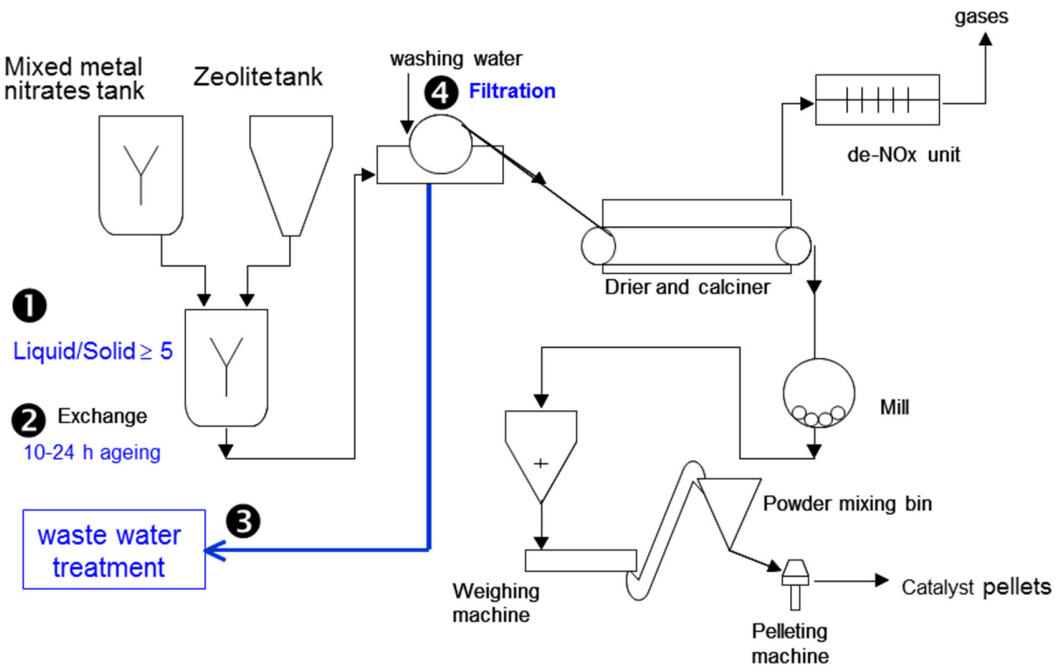

Figure 1. The constraints for the scale-up of a state-of-the-art Fe-Ferrierite N_2O decomposition catalyst are highlighted. The process flow diagram describes the steps of a Fe-exchange zeolite facility highlighting the major bottlenecks: **1**) high volumetric requirements; **2**) long exchange processing times (*i.e.* discontinuous process); **3**) a large volume of generated waste water that needs to be processed before emission, by denitrification based bacterial degradation and **4**) filtration is an energy-intensive and slow process, limited by the zeolite grain size.

Accepted 26/Dec/17 - 10.1021/acs.iecr.7b04584
Final version can be accessed through the ACS website

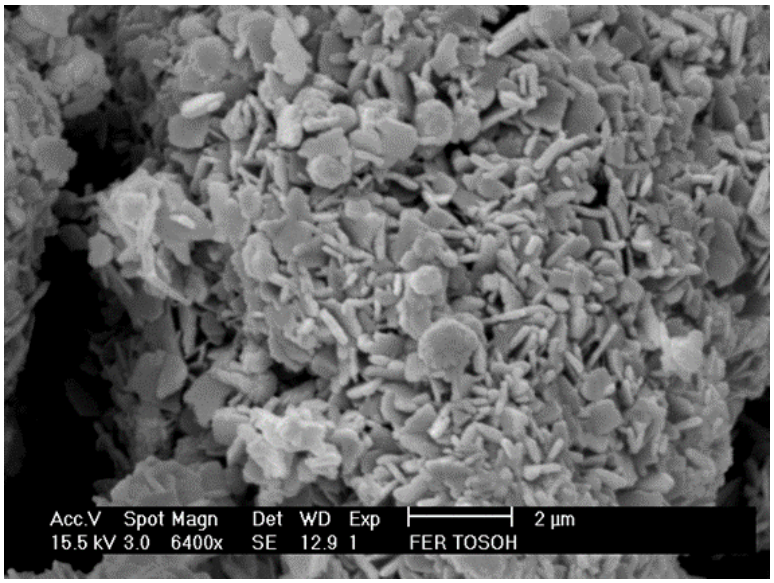

Figure 2. SEM image of the investigated Ferrierite.

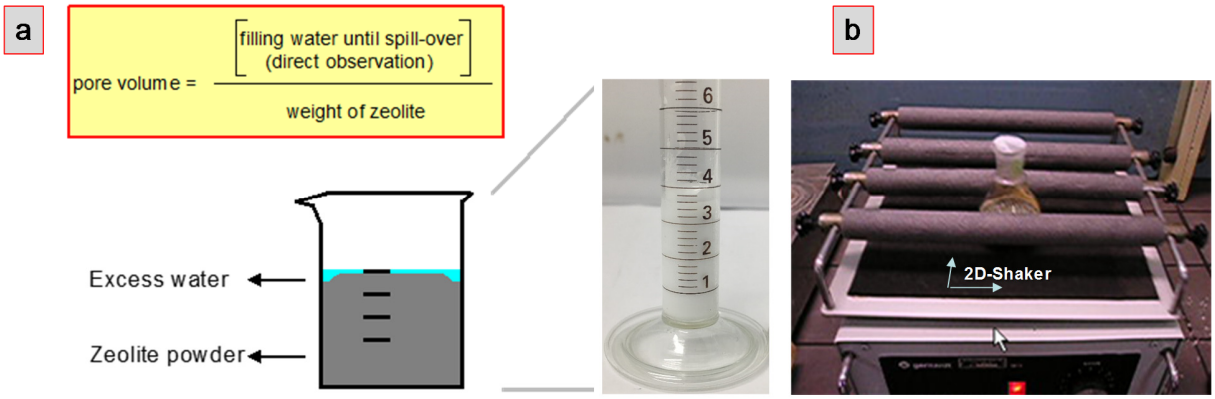

Figure 3. A) Definition of the 'total liquid pore volume' ($V^{T\text{-}LIQ}$). This parameter is determined visually based on the method proposed by Innes.[28] Such values are higher than those determined from gas adsorption. **B**) Experimental set-up used for the dynamic Fe^{3+} exchange of this study. Note that Innes[28] in the original work did not report a graphical illustration of the method.

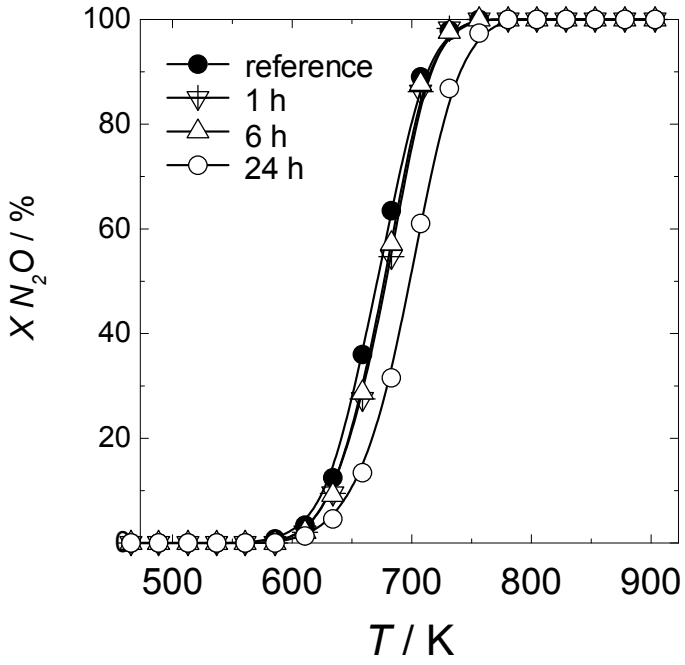

Figure 4. *Static* wetness impregnation for different exchange times. N_2O decomposition conversion as a function of the reaction temperature for 0.5 *wt.%* Fe-FER catalysts prepared under wetness conditions (liquid/solid = 2.5) and the reference standard. Reaction conditions: 3 bar(a) total pressure and W/F = 8.95×10^2 kg·s/mol, He balance.

Accepted 26/Dec/17 - 10.1021/acs.iecr.7b04584
Final version can be accessed through the ACS website

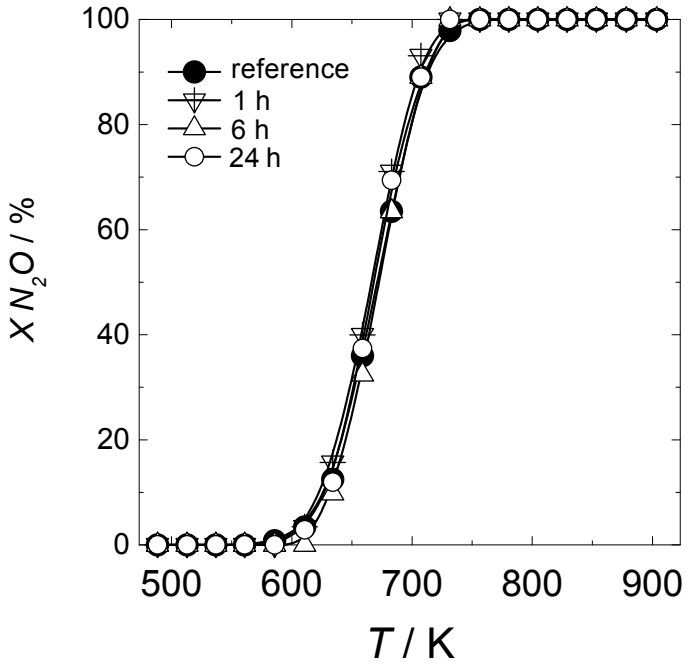

Figure 5. *Dynamic* wetness impregnation for different exchange times. N_2O decomposition conversion as a function of the reaction temperature for 0.5 *wt.%* Fe-FER catalysts prepared under wetness conditions (liquid/solid = 2.5) and the reference standard. Reaction conditions: 3 bar(a) total pressure and W/F = 8.95×10^2 kg·s/mol, He balance.

Accepted 26/Dec/17 - 10.1021/acs.iecr.7b04584
Final version can be accessed through the ACS website

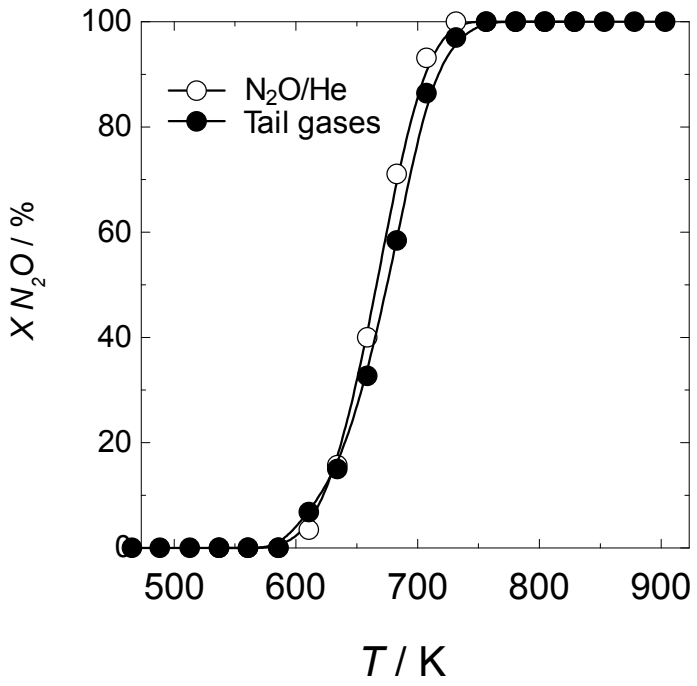

Figure 6. Comparison for the optimal catalyst (dynamic, 1h) under N_2O/He (○, 1500 ppm N_2O) and tail gas conditions (●, 1500 ppm N_2O, 200 ppm NO, 2.5% O_2 and 0.5% H_2O). Reaction conditions: 3 bar(a) total pressure and W/F = 8.95×10^2 kg·s/mol, He balance.

Accepted 26/Dec/17 - 10.1021/acs.iecr.7b04584
Final version can be accessed through the ACS website

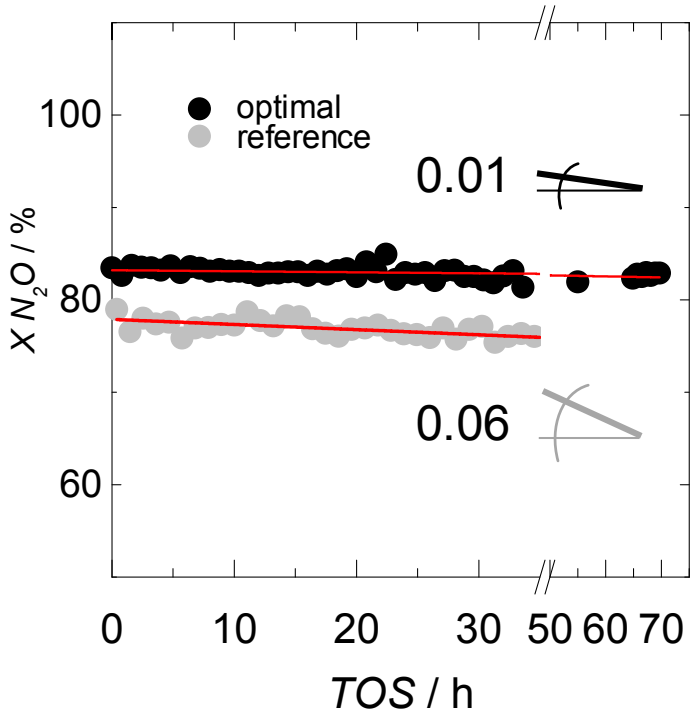

Figure 7. Stability test under tail gas conditions for the optimal (dynamic, 1h) and reference catalysts at 700 K, given as N_2O conversion as a function of the time on stream (TOS). Red lines are the linear regression correlations, and the indicated numbers are the slope as %/h. Reaction conditions: 3 bar(a) total pressure and W/F = 8.95×10^2 kg·s/mol, He balance.

Accepted 26/Dec/17 - 10.1021/acs.iecr.7b04584
Final version can be accessed through the ACS website

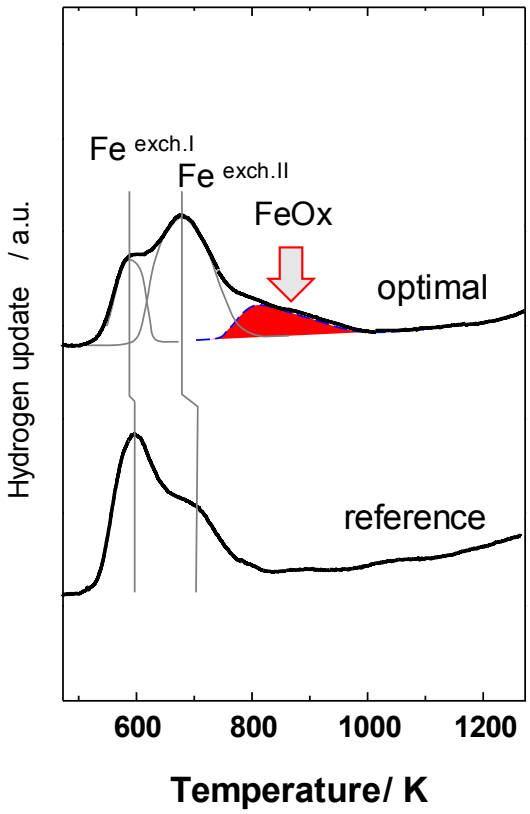

Figure 8. H_2-TPR profiles of the Fe-FER zeolites, optimal (dynamic, 1h) versus reference catalyst. Conditions: H_2/Ar, 10%; ramp: 10 K/min. The FeOx contribution of the optimal catalyst is highlighted to indicate that it is relatively small as compared to what is expected from the thermodynamic values, as discussed in the text.